J Mater Sci (2009) 44:1711–1725
DOI 10.1007/s10853-008-2969-3

Segregation behavior at TGO/bondcoat interfaces

P. Y. Hou

Received: 6 June 2008 / Accepted: 22 August 2008 / Published online: 20 September 2008

Abstract The segregation of sulfur and other elements at the interface between thermally grown alumina and a few coatings have been reviewed and compared with studies made at oxide/metal interfaces formed on model alloys. The coatings studied were NiPtAl on CMSX-4 or AM1 with two different bulk sulfur contents, and NiCoCrAlY on PWA 1484. The segregation behavior at the oxide/PWA1484 interface was also reported. Auger electron microscopy was used to study the chemistry at the oxide/coating interface after portions of the oxide were removed in ultra high vacuum (UHV) by scratches made on the oxidized sample surface. The extent of oxide spallation in relation to the scratch width was utilized to evaluate the interfacial strength, which was then correlated with the interface impurity level. Results showed strong relationship between sulfur segregation and the composition of the alloy substrates. In addition to substrate sulfur content, the degree of sulfur segregation was most significantly increased by Cr co-segregation or decreased by Y doping of the coating. Pt and Hf could stop segregation only when present together. P was found as a significant segregand in one case where sulfur segregation was prevented by Y. These behaviors are discussed in terms of various thermochemical interactions in the bulk and at the interface.

P. Y. Hou (✉)
Materials Sciences Division, Lawrence Berkeley National Laboratory, Berkeley, CA 94720, USA
e-mail: pyhou@lbl.gov

Introduction

Thermal barrier coatings (TBCs) are ceramic coatings that have been successfully applied to the surface of high-temperature metallic components. These coatings create a temperature drop between the operating atmosphere and the metal surface, thus allowing the component to operate at higher temperatures, so that higher efficiency and lower emissions can be achieved. Between the TBCs and the substrate, there is often an oxidation resistant coating, the bondcoat, that oxidizes to form a slow growing α-Al_2O_3 TGO (thermally grown oxide) layer at the ceramic/metal interface. One of the key questions concerning the life-time of TBC systems is whether the ceramic top coat can remain adherent under operating conditions that commonly involve thermal cycling. Spallation of the TBCs is often associated with failure at the TGO/bondcoat interface [1, 2]. Stresses, microstructure, and chemistry at this interface are all important factors dictating the extent of its failure and the failure mechanism. While several other papers in this issue address the failure mechanism and microstructure changes associated with TGO growth, this article deals with the chemical changes that take place at the TGO/bondcaot interface and how the TGO adhesion is affected by these changes.

Sulfur, a common impurity in metals and alloys, can segregate to oxide/metal interfaces during TGO growth or high-temperature annealing. Such segregation of sub-monolayer coverage has been observed experimentally for many model Al_2O_3/alloy systems [3] and for diffusion bonded Ni-sapphire interfaces [4, 5]. Similar to its detrimental effect on grain boundaries, sulfur at the oxide/metal interfaces also significantly reduces the interfacial strength. This effect has been demonstrated experimentally for diffusion bonded systems [5] and for TGO Al_2O_3/alloy

interfaces [3, 6]. First principles calculations have also shown that S segregation to the oxide/metal interface is not only energetically favorable, but also decreases the work of adhesion [7], in agreement with experimental observations.

While the interface segregation behavior has been studied on a number of model Al_2O_3 forming alloys, with results summarized in a recent review [3], much less work has been done on TGO/bondcoat interfaces, where the alloy on which the TGO is formed consisted of at least two layers: an oxidation resistant bondcoat and a superalloy substrate. During high-temperature exposures, components from the two layers will diffuse into each other, changing the bondcoat composition from a 3–5 element system to one that may include all the elements in the superalloy substrate. These extra elements may affect the segregation behavior, such that results found on model alloys may not always be applicable to coatings.

There are two major types of common bondcoats in commercial TBC systems: the overlay MCrAlY type coatings, where M = Ni, Co or both, and the Pt-modified diffusion aluminide coatings, usually of the β-(Ni,Pt)Al phase, but more interests are now placed on the γ/γ'-(Ni,Pt)Al bondcoats, because Pt in the γ/γ' system decreases the chemical activity of Al, thus causing an uphill Al diffusion from the substrate to the bondcoat [8], so that the bondcoat can have ample supply of Al to sustain the Al_2O_3 TGO growth. In the MCrAlY type coatings, Y is added to help improve the TGO adhesion. It is considered a "reactive element", whose function is to improve the oxidation resistance by reducing the Al_2O_3 growth rate and improving the scale adhesion [9, 10]. The way it improves oxide adhesion may be 2-fold: by reducing the S activity in the alloy, thus preventing it from segregating to the interface [3, 11], and by segregating to the interface itself, hence strengthening it [12, 13]. Both of these effects have been demonstrated experimentally on model alloys with Zr [13] and Hf [14] as the reactive elements, and by first principles calculation with Hf [7]. In the aluminide coatings, Pt is added also to improve the oxidation resistance. The beneficial effect of Pt on Al_2O_3 scale adhesion has been known for several decades [15], but the mechanism is still unclear. It has been suggested that Pt additions eliminate interfacial pore formation [16, 17], but this is only true in most but not all cases. In terms of S segregation in NiAl alloy systems, the effect of Pt seems to vary with Al concentration and alloy phases. In off stoichiometric β-NiAl, Pt eliminates interfacial S segregation, and there is no Pt but Al enrichment at the interface [18]. However, in γ or γ'-NiAl, Pt only reduces the degree of S segregation but not eliminate it; the interface is slightly enriched with Pt, but not Al [3, 14].

In this article, limited experimental studies to date on the segregation behavior at TGO Al_2O_3 and bondcoat interfaces will be presented and discussed. These include β-(Ni,Pt)Al bondcoats on three different single crystal Ni-based superalloys and one NiCoCrAlY coating on PWA 1484. These results will be compared with segregation studies made on model alloys to evaluate the effect of superalloy substrate components on segregation and any synergisms between segregating elements.

Experimental procedure

The β-(Ni,Pt)Al bondcoats, on two types of single crystal Ni-based superalloys: AM1 and CMSX4, were deposited by platinum electroplating followed by low-activity CVD aluminizing [19]. On the CMSX4, a NiAl coating without the Pt was also deposited and studied for comparison [20]. The superalloy compositions are listed in Table 1. Bondcoats on two AM1 alloys were examined: one had a common S level of 4 ppm, the other only 0.2 ppm. They are referred to, respectively, as standard-S (s-S) and low-S (l-S) alloys. The initial coating thicknesses were between 50 and 60 μm. They consisted of an outer single-phase aluminide layer with an average composition of 37 Ni, 11 Pt, and 45 Al (in at.%), and an inner multi-phase diffusion zone; the coating surfaces had a distinct network of grain-boundary ridges. These features are typical of outward-growing CVD nickel aluminides [16].

A NiCoCrAlY coating deposited on PWA1484 was also studied. The substrate composition is given in Table 1. The bondcoat, ~100 μm in thickness, consisted of (in at.%) 40.4 Ni, 18.8 Co, 16.4 Cr, 23.3 Al, 0.3 Y, 0.1 Hf, and 0.7 Si [21]. It was deposited by vacuum plasma spraying and subsequently shot peened and then treated with a standard densification heat treatment at Pratt and Whitney, USA.

Tests coupons, cut to about 10 × 10 mm, were oxidized in laboratory air between 1,050 and 1,150 °C with fast cooling, where the samples were pulled out of the furnace after their desired oxidation times. Other than those on the AM1 substrate, where the bondcoat surface was polished to a 1 μm finish with diamond paste, the samples were used in their as-received state. All samples were cleaned ultrasonically in acetone and then ethanol before oxidation.

Interfacial chemical analyses were performed using a PHI 660 Auger microscope. To expose the interface, the oxidized sample surface was scratched with a Vickers micro-indenter that was specifically designed and mounted on a linear translator inside the ultra high vacuum (UHV) chamber of the microscope [3, 22]. Scratches made this way, when applied with sufficient load, caused pieces of the oxide film around the scratch to spall; an example can be seen in Fig. 8b. The scale/alloy interface was exposed if adhesive failure took place. The method is similar to a scratch adhesion test done under constant load, where the

Table 1 Chemical composition of the three types of single crystal Ni superalloys on which bondcoats were deposited

Alloy type	(at.%)									(ppma)			
	Ni	Al	Cr	Co	Ta	W	Mo	Ti	Re	Hf	Y	Zr	S	C
AM1	68.1	12.3	9.3	7.2	2.8	2	1.8	1.8	–	–	–	–	0.2, 4	108
CMSX4	63.1	12.9	7.4	9.8	2.2	2.1	0.4	1.3	1	0.03	<1	13	4	101
PWA1484	63.2	13	6	10.6	3	2	1.3	–	1	0.035	–	–	10–16	

scratch width is proportional to the load and the extent of spallation is related to the interface strength. The ratio of the width of a scratch over the width of spalled areas around that scratch, therefore, was used as a measure of the relative interface strength of different samples.

The exposed alloy surfaces were analyzed using a 0.5–1 μm AES probe, whether on oxide imprinted areas, where the oxide was in contact with the alloy prior to the scratch, or on the surface of interfacial voids. Some of the oxide pieces that spalled from the scratch motion would flip over, allowing the oxide side of the interface (the scale underside) to be examined. These locations always consisted of only O and Al, so segregands at the interface, if any, all resided on the alloy side after scale spallation. Compositions of the bulk alloys were obtained from analyses made along the center of the scratch where the indenter had removed the entire surface scale and plowed into the alloy.

Results

Segregation on β-NiAl and NiPtAl coatings on CMSX4

Due to the high-temperature aluminizing process, elements from the substrate diffused into the coating, such that the outer layer of both types of coatings also contained small amounts of Co, Cr, Ti, and Re, and the inner layer was slightly enriched with W and Ta [20]. Coated samples, in its as-received condition after cleaning, were oxidized at 1,150 °C isothermally for 10, 100, or 250 h, or under 2,000 10-min cycles. The alumina scales that formed on the Pt-containing coating remained adherent even after the cyclic oxidation testing, but spallation during cooling was

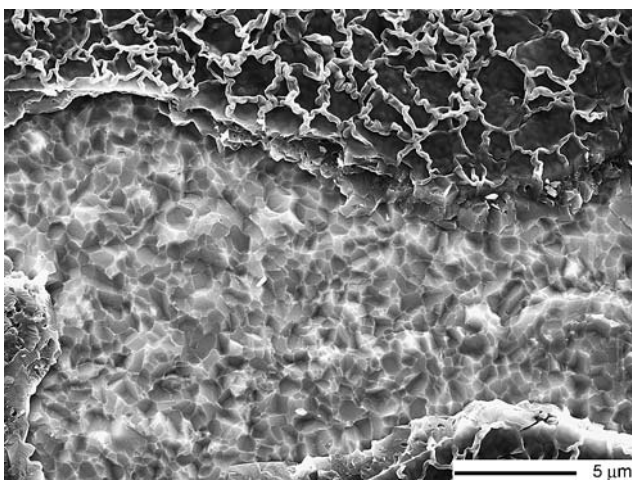

Fig. 1 SEM micrograph of a scratch-induced spallation area on NiAl deposited on CMSX4 after 1,150 °C oxidation for 10 h (courtesy V.K. Tolpygo [20])

observed on the NiAl coating after 100 h isothermal oxidation and sample weight loss became noticeable after 600–700 cycles [20].

Oxide scales on the NiAl coating can be easily scratched off, even on the 10 h sample where spontaneous spallation during cooling did not take place. Figure 1 shows an interface area on this sample after portions of the scale spalled from the scratch motion. No voids were detected anywhere; the interface consisted of imprints no more than 1 μm in size made by grains of the TGO film. Auger analyses on several different areas of the interface all showed a small amount of sulfur, with an average surface concentration of 0.9 ± 0.3 at.%, which amounts to approximately 0.1–0.2 monolayer based on attenuation of the Ni peak. An example of the interface composition is shown in Fig. 2a. Compare to the composition of the bulk coating (Fig. 2b), obtained from analysis made on the bottom of the scratch track, the interface is seen to be enriched not only with S, but also N, Ti, Cr, and possibly Co as well. The oxygen and carbon are usual UHV contaminants, since their levels increased with exposure time in the AES chamber. A group of peaks (marked by the arrow in Fig. 2a) with energies close to that of Ta, W, and Re were consistently present. Closer examination of the peak energies seemed to suggest that they may correspond to Rhenium. Nano-sized Re [16] and Cr [16, 23] particles at Al_2O_3/NiPtAl interfaces have been previously detected by TEM, but their fraction at the interface is not known.

After longer isothermal exposures (100 and 250 h), extensive scale spallation took place on the NiAl coating almost exclusively along coating grain-boundary ridges, whether or not there were interfacial voids that formed preferentially on them [20]. Figure 3 shows the location and morphology of one of these voids on the 100 h sample. Auger analysis on oxide imprinted areas (those surrounding the voids and similar to that shown in Fig. 1) again detected small amounts of sulfur, at 1.1 ± 0.4 and 0.9 ± 0.3 at.%, respectively for the 100 h and 250 h samples. Other than S, the interfaces were also enriched with other elements like those found on the 10 h sample. Variations of the interface concentrations of S, N, Ti, Cr, Co, Ni, and Al with oxidation time are illustrated in Fig. 4, and compared with those detected within the coating. Concentrations were calculated from differentiated Auger peak heights and tabulated sensitivity factors [24]. Since these factors were not calibrated for the current system, the

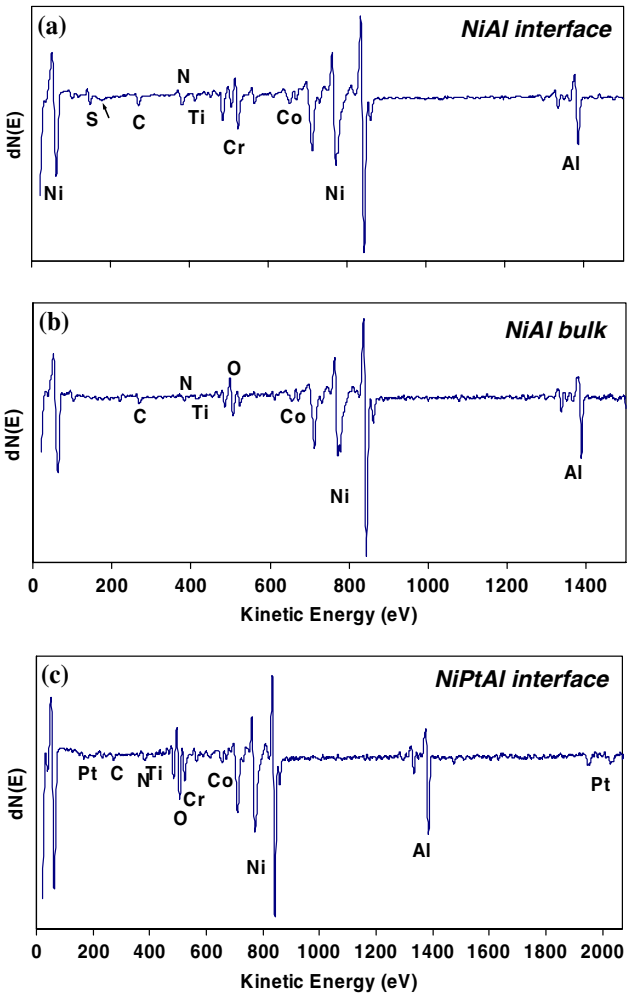

Fig. 2 Typical AES spectrum after scratching and TGO spallation on (**a**) NiAl coating interface (**b**) NiAl coating within scratch mark, and (**c**) NiPtAl coating interface. Both coatings deposited on CMSX4 and oxidized at 1,150 °C for 250 h

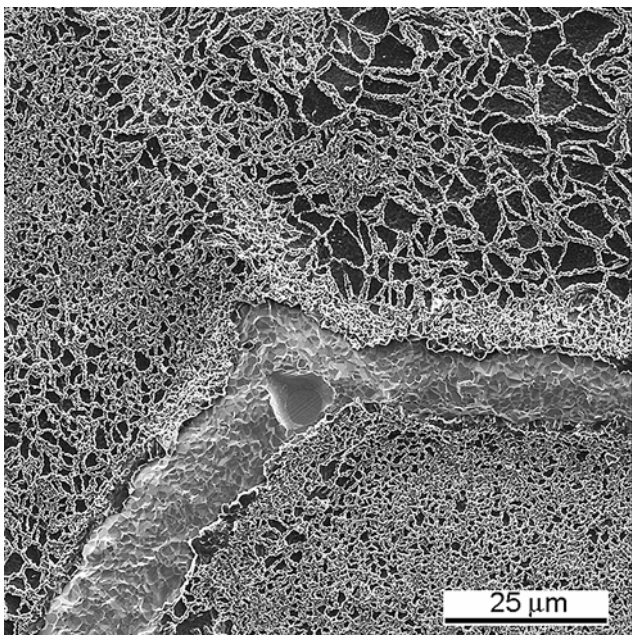

Fig. 3 SEM micrograph showing preferential TGO spallation and interfacial void formation on grain-boundary ridges of the NiAl coating on CMSX4 after 100 h oxidation at 1,150 °C (courtesy V.K. Tolpygo [20])

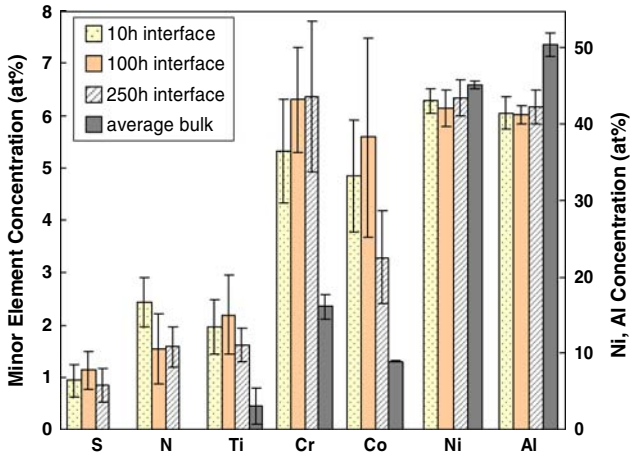

Fig. 4 Variation of interface composition with oxidation time (at 1,150 °C) on the NiAl coating on CMSX4 compared with compositions within the coating

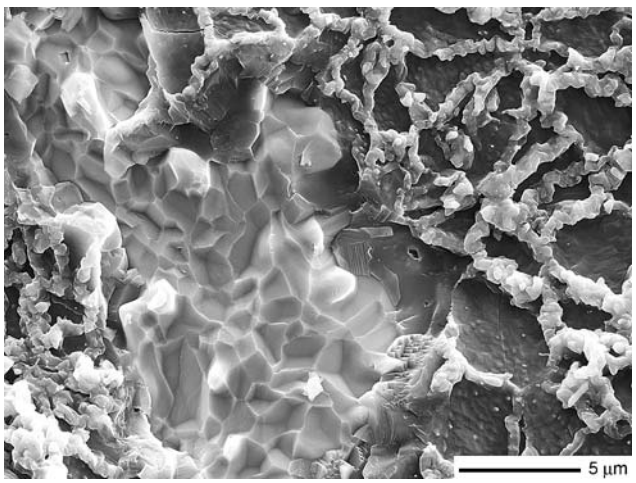

Fig. 5 SEM micrograph of a scratch-induced spallation area on NiPtAl deposited on CMSX4 after 250 h 1,150 °C oxidation (courtesy V.K. Tolpygo [20])

results of some elements may have systematic errors. Figure 4 clearly shows that S and N segregated to the interface while Ti, Cr, and Co were also enriched there. The interfacial Al level was consistently lower than that in the bulk, most likely due to Al consumption by oxidation. Within experimental errors, all elements showed no variations with oxidation time, indicating that the interface composition was already at a steady state after 10 h at 1,150 °C. Occasionally, P, Si and/or Ca were also detected, but their levels were always low, <1 at.%. Of all the areas analyzed, 23% contained P, 2% had Si and 4% had Ca; there was no apparent relationship between these frequencies with oxidation time.

Interfacial voids were only observed on the 100 h and 250 h samples. Most of the void surfaces were covered with a thin layer of oxide, due to spallation or cracking of the scale above the voids during cooling. Only one void was found to be oxide-free during the AES investigation, and its sulfur content, up to 15 at.%, was significantly higher than that found on the interfaces. This high concentration on the void face is similar to that found on binary model Ni-40Al and Ni-22Al alloys, where the sulfur contents on their void faces were 8–12 and 14 at.%, respectively [3]. These concentrations are close to a full monolayer at the NiAl surface.

The oxide scales on the NiPtAl coating were much more difficult to scratch off, indicating strong interface adhesion. Scratching only induced small areas of spalls (Fig. 5 is an example), which showed oxide imprints with no voids. Contrary to the NiAl coating, no sulfur was detected at the Al_2O_3/NiPtAl interface (Fig. 2c). Due to the presence of a group of low-energy Pt Auger peaks between 150–250 eV, the detection limit for S, at ~0.2 at.%, was twice as high as that on NiAl. These peaks also overlapped with those of Re, W or Ta, which appeared on the NiAl coating. Table 2 summarizes the average compositions found at the TGO/NiPtAl coating interface and compared them with that detected inside the coating. Similar to the NiAl coating, the interface was slightly enriched in Ti, Cr, and Co, depleted in Al and contained N. Unlike NiAl, the Cr and Co enrichment was much lower; there was also no S, as stated earlier. The Pt concentration seems to be slightly higher at the interface. Similar enrichment has been found on γ and γ'-NiPtAl alloys [3, 14], but not on β-NiPtAl [3, 18], where instead an Al enrichment was present. With these limited results (also see Fig. 12), it appears that Pt segregates to the oxide/metal interface only when it is not enriched with Al.

At a few locations, on the NiPtAl as well as the NiAl coating, high levels of Cr, from 14 up to 40 at.%, were detected, but were not included in the average concentration calculation. These areas may be at or close to a Cr-rich precipitate at the interface.

Table 2 Concentration (in at.%) from Auger analysis of the NiPtAl bondcoat on CMSX4 and the bondcoat/Al_2O_3 interface. Data averaged over samples oxidized from 10 to 250 h at 1,150 °C

	S	N	Ti	Cr	Co	Ni	Al	Pt
Inside coating			0.4 ± 0.4	2.0 ± 0.3	1.5 ± 0.2	39.3 ± 5.7	50.2 ± 0.2	4.8 ± 0.7
At interface	<0.2	1.6 ± 0.3	1.2 ± 0.4	4.0 ± 0.2	1.9 ± 0.1	36.1 ± 0.7	48.1 ± 0.1	6.8 ± 1.1

Segregation on β-NiPtAl coatings on standard and low-S AM1

Before oxidation, the external β-NiPtAl layer of the coating also included 4.6, 1 and 1 at.% of Co, Cr, and Ta, respectively, which have diffused into the coating from the substrate during the aluminizing process [25]. Surfaces of the as-received coatings were lightly polished to a 1 μm finish before oxidation at 1,100 °C in air for 1, 10, and 50 h. Detailed characterization by TEM of the microstructural changes of the coating deposited on the standard-S alloy has been published [23, 26]. After 1 h, the outer layer of the coating remained a single β phase, but contained TCP phases along some grain boundaries and at triple-grain junctions. With longer exposures, as the coating Al content decreased, the γ' (Ni_3Al) phase started to form preferentially at β/β grain boundaries and within the β grains as platelets. Its volume fraction increased with oxidation time. After 50 h, grain boundaries of the outer layer has completely transformed into the γ' phase, and some γ' gains also existed at the TGO/BC interface; examples of these morphologies are shown in Fig. 6. It is seen in this figure that many small Cr particles were present within the β grains. Most of them precipitated next to the γ' platelets; some were also found at the TGO/bondcoat interface. The majority of these particles are believed to have precipitated during cooling, since their volume fraction greatly decreased when the oxidized sample was cooled by quenching in water rather than in ambient air [27]. Similar development of the oxide and coating morphology was also observed on coatings deposited on the low-S alloy [27].

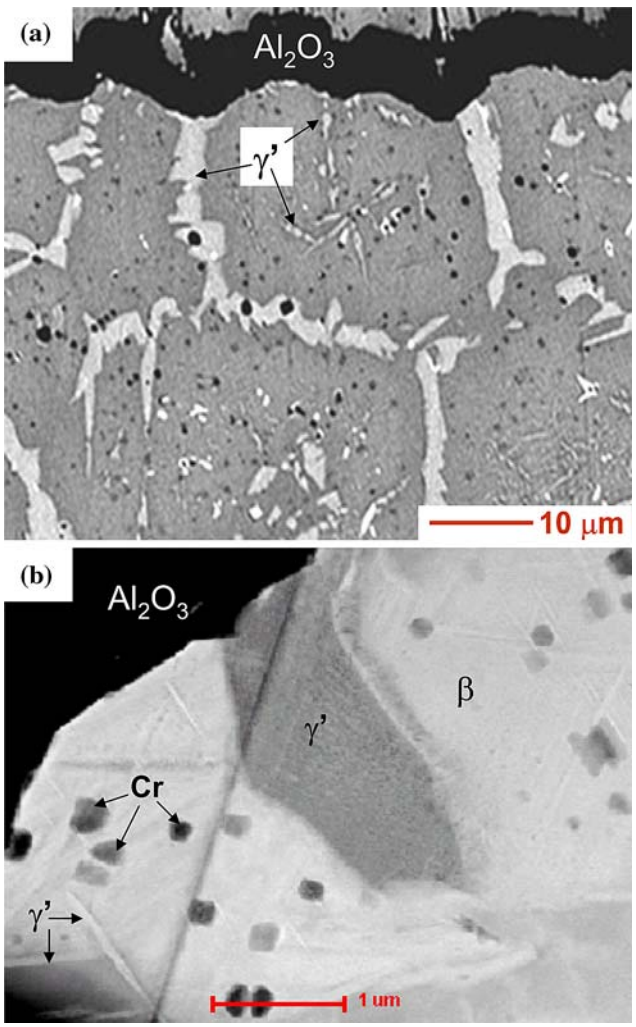

Fig. 6 Morphology of outer NiPtAl coating on standard-sulfur AM1 after 30–50 h oxidation at 1,100 °C, (**a**) SEM and (**b**) TEM images (courtesy R. Molins [23])

Analytical STEM analysis performed with coatings on the standard-S alloy [23, 26] have shown the presence of sulfur at the following locations: around the Cr and TCP precipitates in the β phase, at β/β grain boundaries and γ'/β phase boundaries and at γ'/TGO and Cr/TGO interfaces. However, no S was detected by TEM at the TGO/β interfaces. It is important to note that the Cr particles were identified by diffraction as α-Cr. Sulfur was always found next to the Cr particles, but not within them, indicating that they were not chromium sulfides. Figure 7 is a clear demonstration showing S segregation around a Cr particle that had precipitated at the TGO/coating interface. Some of the Cr particles were also enriched with Co and Mo. Other segregands that have been detected by TEM were Cr and Co at γ'/γ' grain boundaries and Cr, along with S, at the γ'/β interface.

Unlike the NiPtAl coating deposited on CMSX4, the Al_2O_3 scale formed on this bondcoat showed severe spallation. The degree of spalling increased with oxidation time. Interfacial voids were numerous, and their average size and surface fraction in the spalled areas increased with time [26]. Figure 8a gives an example of the large interface voids that formed after 50 h oxidation. In contrast, Al_2O_3 scales on bondcoats deposited on the low-S substrate did not show any spallation during cooling [28]. Even so, the oxide layer could be scratched off relatively easily (Fig. 8b); the interface contained no voids, only oxide imprinted areas (Fig. 8c).

With the coating deposited on the standard-S alloy, sulfur was detected at the TGO/coating interface (oxide imprinted areas) and on interfacial void faces. The amount on voids was quite low after 1 h (Fig. 9), but quickly reached a steady state level of ~15 at.% from 10 to 50 h. The amount on interfaces also built up slowly with time, but the level was always less than that found on voids. By 50 h, experimental data could be separated into two distinct groups based on their sulfur concentrations, which averaged 2 and 12 at.%, respectively. The high-sulfur areas

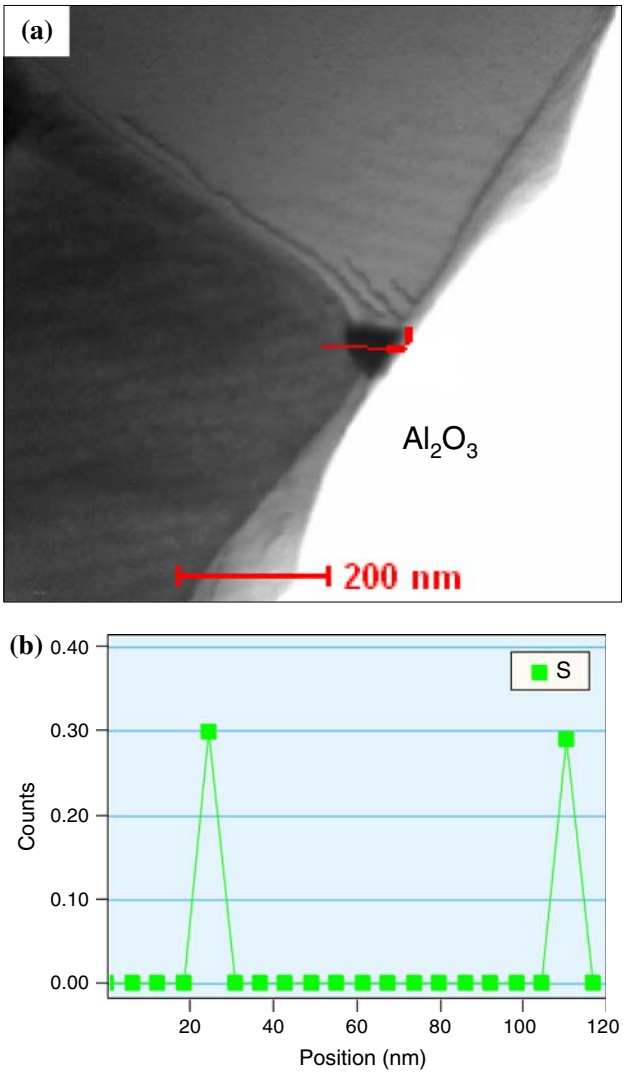

Fig. 7 (**a**) Cross sectional TEM micrograph of NiPtAl coating on standard-sulfur AM1 after 32 h oxidation at 1,100 °C, showing Cr precipitate at the TGO/coating interface. (**b**) Corresponding EDS-STEM line profile showing S enrichment around the particle (courtesy R. Molins [23])

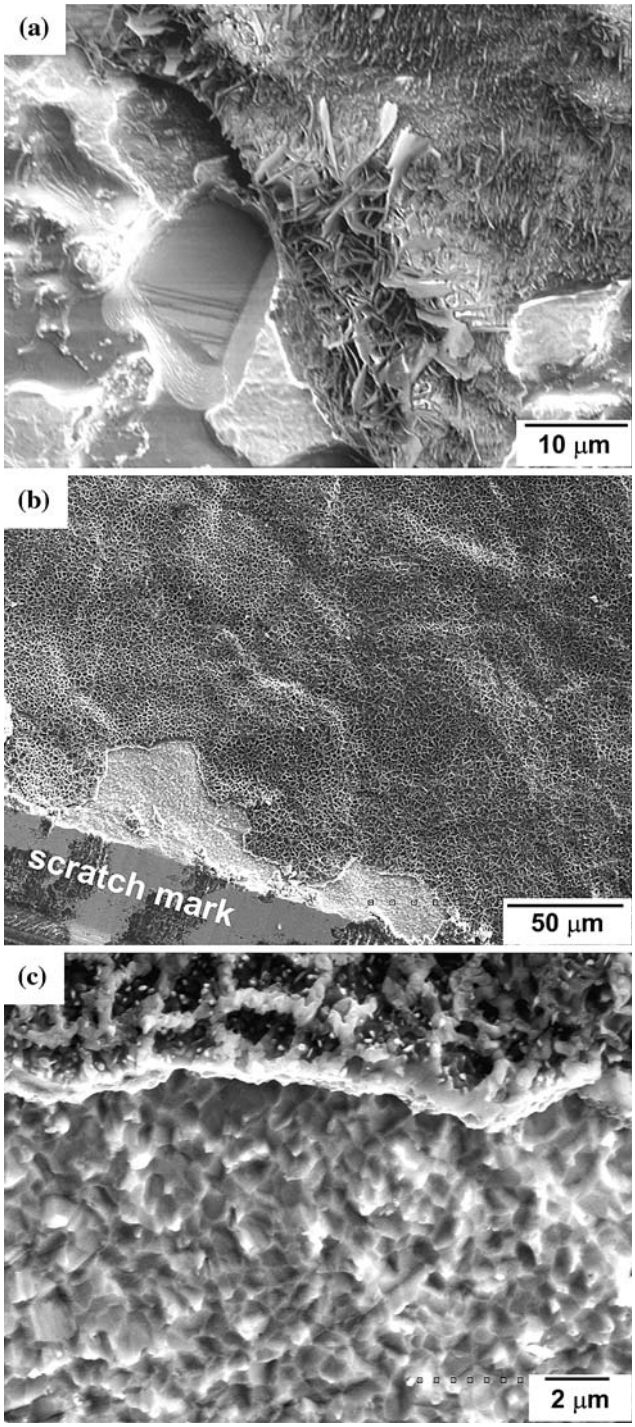

Fig. 8 SEM images of NiPtAl coating after 50 h at 1,100 °C on (**a**) standard-sulfur AM1 (courtesy R. Molins), and (**b**), (**c**) low-sulfur AM1

have been shown to be associated with the tiny Cr precipitates or the γ' phases at the TGO/bondcoat interface [26]; distributions of these features can be seen in Fig. 6. Auger line scans taken across bondcoat grains showed higher levels of S at the grain boundaries; an example is given in Fig. 10. Along the line were other areas high in S. These may be patches of γ' phases present at the interface, or areas near Cr particles that were too small to be resolved by a conventional SEM. While no apparent relationship existed between the amount of S and other elements at the interface, S and Cr were found to increase concomitantly. This relationship is illustrated in Fig. 11, where the Auger peak heights of S and Cr, normalized by that of Ni, are plotted against each other. Depth profiles through the interface area always showed that Cr was located immediately beneath the surface sulfur. One such example from the 1 h sample is given in Fig. 12. After this short oxidation time, the coating in contact with the TGO was still β-NiPtAl without any γ' phase or Cr precipitates [23, 26]. This Cr enrichment, therefore, must not have

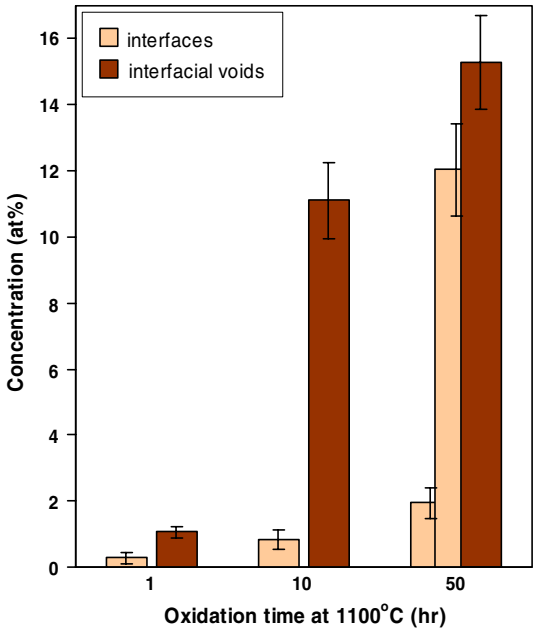

Fig. 9 The build up of sulfur with time on a NiPtAl coating deposited on standard-sulfur AM1, after TGO removal in vacuum

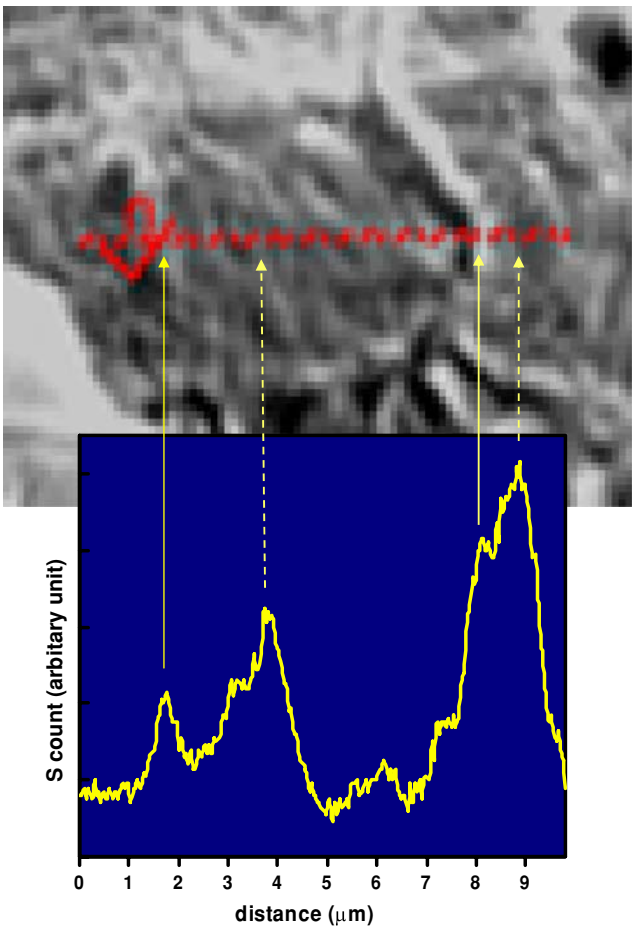

Fig. 10 SEM image and Auger sulfur line scan across a NiPtAl grain deposited on standard-sulfur AM1 after its 1,100 °C–50 h TGO was removed in vacuum

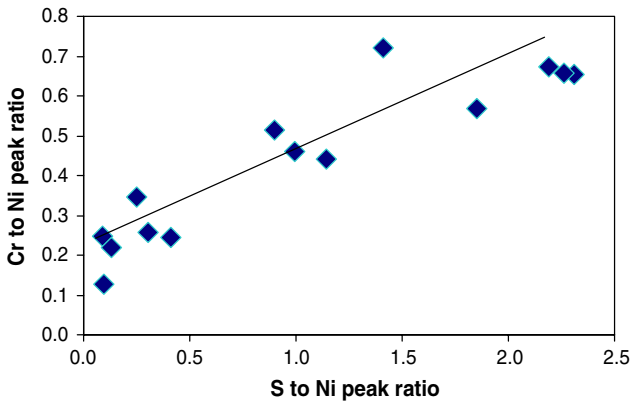

Fig. 11 Auger peak height ratios of Cr/Ni versus S/Ni showing a relationship between S and Cr segregation. Data points from the 1,100 °C–50 h NiPtAl/standard-sulfur AM1 sample

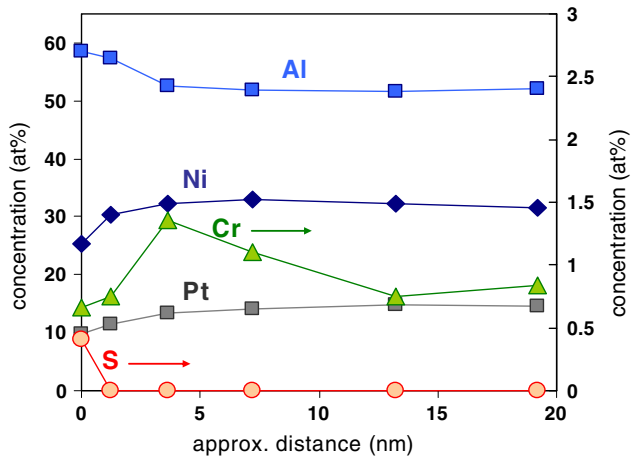

Fig. 12 Auger depth profiles through NiPtAl coating deposited on standard-sulfur AM1 after TGO (1,100 °C–1 h) removal in vacuum

come from a particle, but was Cr segregated near the interface. The Al concentration was higher at the interface, but there was no Pt enrichment at or near the interface, similar to results on Al_2O_3/alloy interfaces formed on model NiPtAl alloys [18].

An Auger spectrum from one of the low-S regions on the 50 h sample is shown in Fig. 13a. Other than the coating elements (Ni, Al, and Pt) and S, nitrogen, titanium, chromium and cobalt were also present. Occasionally, low levels of P or Si (less than 1 at.%) were found. Of all the areas examined, 18% had P and 25% had Si. Figure 13b shows a typical spectrum taken from the coating deposited on the low-S alloy. Although oxidized under the same condition as the sample shown in (a), these interfaces did not display any noticeable amount of sulfur, nor P or Si. The interface sulfur content, if any, should be less than the detection limit of 0.2 at.%. The two spectra in Fig. 13 demonstrated that the type and

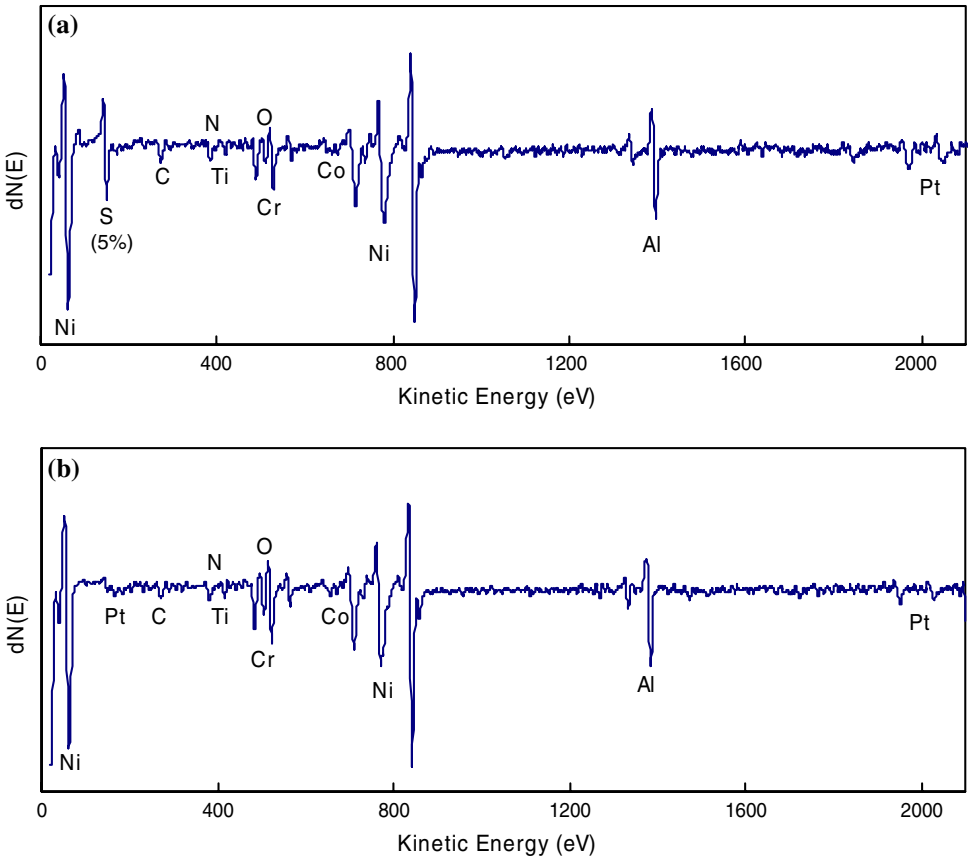

Fig. 13 Typical AES spectrum on NiPtAl surfaces after scratching and TGO (1,100 °C 50 h) spallation; coating deposited on (**a**) standard-sulfur AM1, with the S concentration in at.% noted, and (**b**) low-sulfur AM1

level of all interfacial elements, other than S, were similar for coatings deposited on the standard or the low-sulfur substrates. In other words, the substrate sulfur concentration only affects the degree of S segregation, but not the overall interface composition.

Segregation on PWA1484 and on the NiCoCrAlY coating deposited on it

The vacuum plasma sprayed NiCoCrAlY is a two-phase γ and β coating. Nano-sized spherical γ'-Ni_3Al precipitates are present in the γ phase. The γ' precipitates are richer in Ni and Al, but Cr and Co partition preferentially to the γ matrix [29]. The coating oxidizes to form an alumina TGO. After exposure at 1,100 °C for 100 h isothermally, a layer of γ, about 3 μm thick, is developed immediately below the TGO due to Al depletion [29].

The coated sample was cut such that one main face of each test specimen was the coating while the other side exposed the superalloy substrate. The substrate surface was polished on SiC paper, but the coating surface was untouched. Each specimen was cleaned prior to oxidation. Three isothermal oxidation conditions were used: 1,050 °C for 100 h, 1,100 °C for 100 h, and 1,100 °C for 2.5 h followed by 1,050 °C for 97.5 h. In all cases, noticeable oxide spallation took place on the substrate surface after cooling. Only small areas of spalls were observed on the coating surfaces, with the 1,050 °C sample showing the most spalls. The TGOs that formed on the coating or the superalloy were always Al_2O_3. The oxide scale consisted of thick and short platelets (after 1,100 °C or 1,100 then 1,050 °C) or long and thin whiskers (after 1,050 °C) on its surface, beneath which was a thin layer of fine equaxed grains, followed by a columnar grain layer at the oxide/metal interface. An example of the 1,100 °C scale is illustrated in Fig. 14a.

Spallation of TGOs on the coating and the superalloy side both took place at the oxide/metal interface regardless of whether it happened during cooling or scratching. A few interfacial voids were observed on the specimen oxidized at 1,050 °C. Spalled areas on all other samples showed only oxide imprinted areas. On the coating side, broken pegs were often observed on the metal surface; an example is given in Fig. 14b with a near circular peg in the center surrounded by oxide imprinted coating surface. The presence of these pegs, which were internal oxides that grew preferentially along reactive element-rich particles in the alloy [30], has been well documented; examples of their cross-sections can be found in references [31] and [32]. From Fig. 14b, the peg is seen to consist of an outer layer

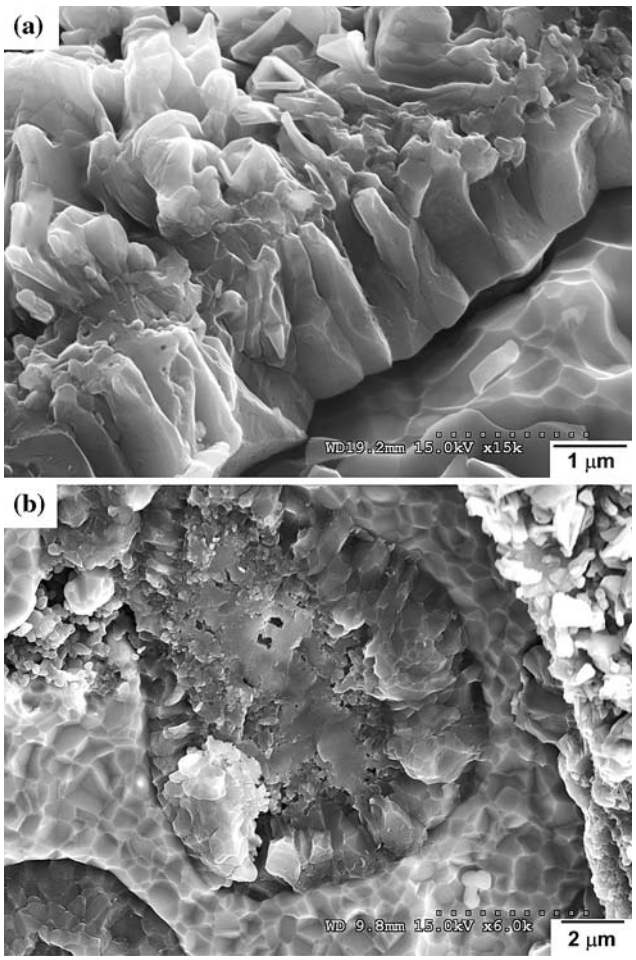

Fig. 14 SEM images from the NiCoCrAlY coating after 100 h at 1,100 °C, showing (**a**) a fractured cross section of the TGO and (**b**) a broken peg at the coating surface surrounded by TGO grain imprints

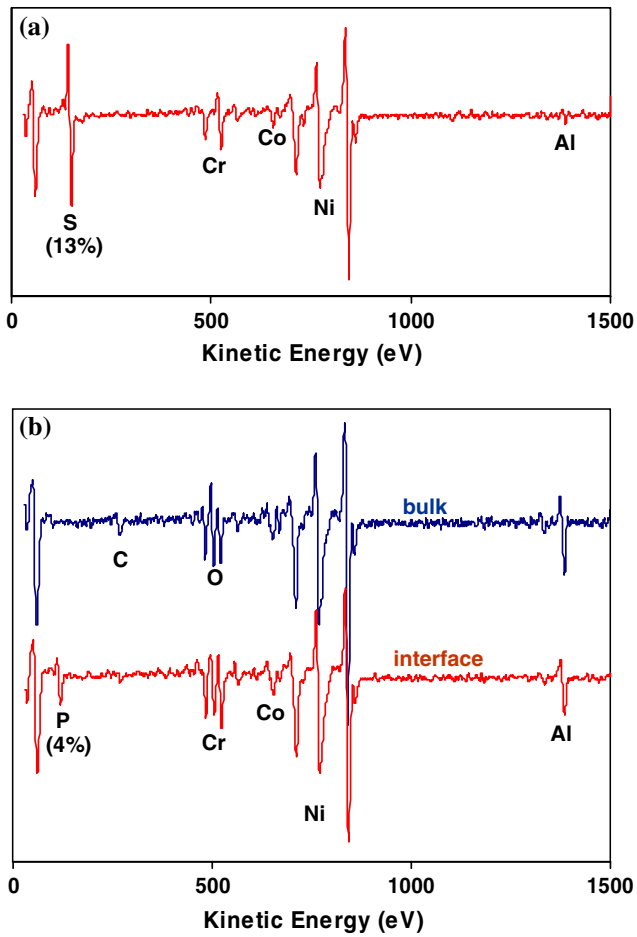

Fig. 15 Typical AES spectrum on surfaces of (**a**) PWA1484 and (**b**) NiCoCrAlY coating on PWA1484, after TGO removal in vacuum. Oxidation was carried out at 1,050–1,100 °C for 100 h. The S and P concentrations in at.% are noted

of Al_2O_3 and a less dense inner core, which had been shown to contain Y, Hf, and S [33].

Sulfur was detected everywhere at the TGO/PWA1484 interface, with an average concentration of 12.7 ± 1.5 at.%. 20% of the examined interfaces also had ~3 at.% P, but S was clearly the most dominant segregand. A typical Auger spectrum of these interfaces is shown in Fig. 15a. Other than an obvious enrichment of S, the interface was also slightly enriched in Co and Cr, by about 2 at.%, and depleted in Al by ~3 at.%.

At the TGO/NiCoCrAlY interface S was never detected, where the detection limit was better than 0.1 at.%. Instead, P was found every time an oxide imprinted region was examined. Figure 14b compares the Auger spectra from the TGO/NiCoCrAlY interface and from within the depth of the scratch. P is seen to be a segregand at the interface. Other than a slight Al depletion, by about 2 at.%, the interface composition was similar to that of the bulk. The P concentration, averaged over every oxide imprinted areas analyzed on samples oxidized under all three conditions, was 3.6 ± 1.6 at.%. Its level varied from point to point between 2 and 8 at.%, but there was no apparent association with oxidation temperature or any noticeable interface morphology. On the few void faces, found after 1,050 °C oxidation, the average P content was 5.0 ± 1.5 at.%, which was similar to that found at the interface. But unlike the interface, a small amount of S, 1.0 ± 0.6 at.%, was detected on interfacial voids. A summary of the P and S concentrations on these interfaces and void surfaces is given in Fig. 16.

Relationship between segregation and interfacial strength

The interfacial strength of each tested sample was evaluated by taking the ratio of the width of a scratch over the width of spalled areas around that scratch, since both widths increased with increasing loads. Figure 17 shows

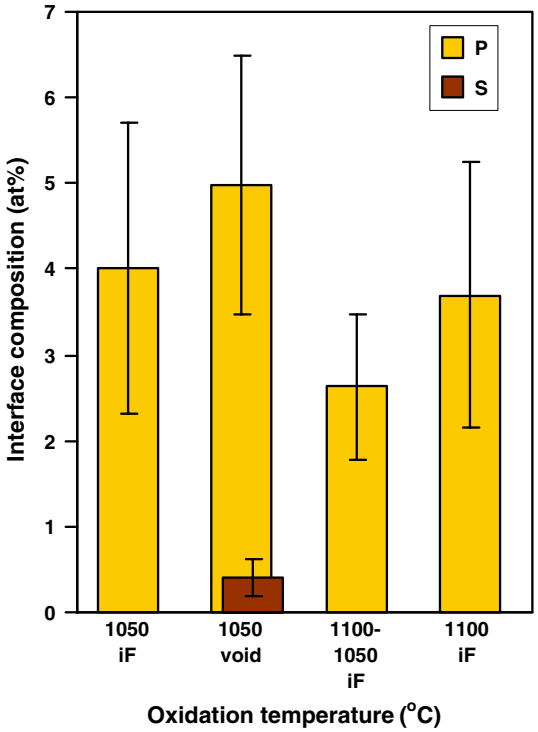

Fig. 16 The amount and type of impurity found on TGO/NiCoCrAlY interfaces (oxide imprinted areas) or interfacial void surfaces after 100 h oxidation at different temperatures

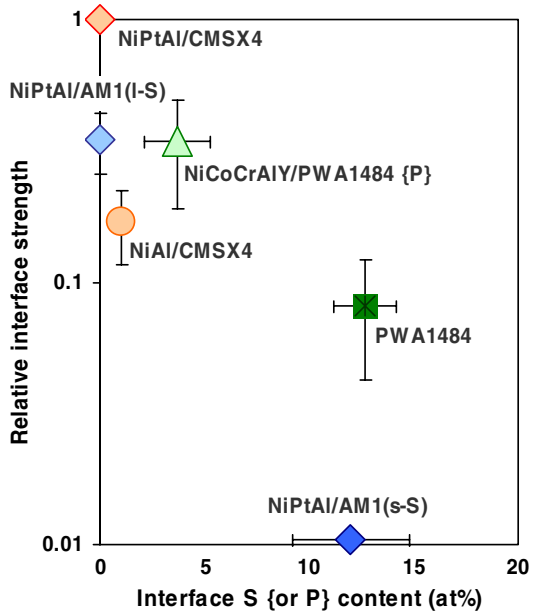

Fig. 17 Comparison of interfacial strength with interface impurity levels. Phosphorus was found on the NiCoCrAlY; every other sample had sulfur at the interface

the relationship between thus determined interface strength and the amount of S or P detected at the interface. The NiCoCrAlY coating was the only sample with P as the dominant segregand; all others had S. The interface strength was normalized with that obtained from the strongest interface of this group of tested samples, i.e., the one formed on the NiPtAl coating on CMSX4. It is seen that in general, the higher the sulfur contents at the interface, the lower the interfacial strengths, and the presence of P seemed less detrimental than S in affecting the strength. However, other factors, such as interfacial void density and other segregands, particularly reactive elements, must also have played a role. Two examples of these extra factors can be seen here. One is between the PWA1484 substrate and the NiPtAl coating on the standard-S AM1. Both have similar amounts of interface sulfur, but the high number of voids on the latter gave rise to a much weaker interface. Another is between the NiPtAl coatings on the CMSX4 and the low-S AM1 alloys. While no S above background levels were detected on neither TGO/coating interfaces, the latter was obviously weaker. Reasons for these differences and the possible effects of other segregands will be elaborated in the discussion section.

Discussion

The amount of sulfur found at different bondcoat/TGO interfaces and at one substrate superalloy/TGO interface is summarized in Fig. 18. Table 3 lists the steady state levels of segregated S or P at oxide-imprinted interfacial areas and on voids, and compares them to scale adhesion, expressed as relative interfacial strengths. In terms of segregation, the following conclusions can be drawn.

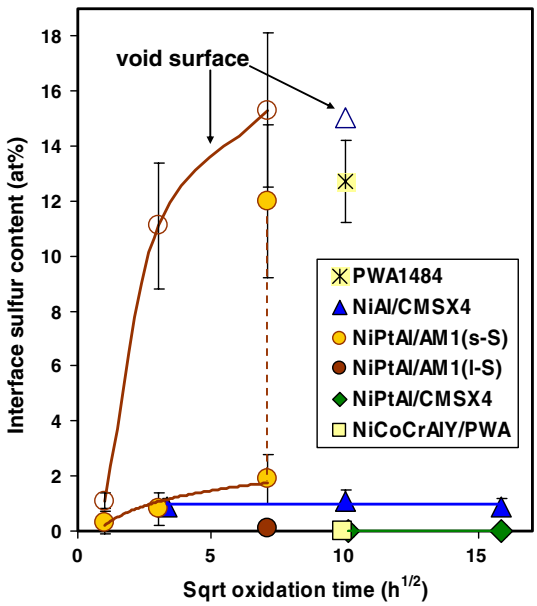

Fig. 18 Summary of the amount of sulfur found on different TGO/coating or TGO/alloy interfaces after oxidations between 1,050 and 1,150 °C

Table 3 Sulfur or phosphorus concentration at Al_2O_3/coating or alloy interfaces and its effect on scale adhesion; oxidations performed at 1,050–1,150 °C with times from 50 to 250 h

Coating	Substrate	Bulk S content (ppm)	S_{iF} (at.%)	S_{void}	$P_{iF}{}^{+}$	P_{void}	Relative strength (%)
NiAlPt	AM1 (std-S)	4	1.9 ± 0.9, 12.0 ± 2.8	15.3 ± 1.9	0.2 ± 0.4, 0.5 ± 0.6	1.3 ± 0.1	<1
None	PWA1484[a]	10	12.7 ± 1.5	–	0.6 ± 1.3	–	8 ± 4
NiAl	CMSX4[a]	4	1.0 ± 0.3	15.0	<0.1	<0.1	17 ± 5
NiAlPt	AM1 (low-S)	0.2	<0.2	–	<0.1	–	35 ± 9
NiCoCrAlY	PWA1484[a]	10	<0.2	1.0 ± 0.6[b]	3.7 ± 1.6	5.5 ± 2.7	34 ± 15
NiAlPt	CMSX4[a]	4	<0.2	–	<0.1	–	100

[a] Alloy contains Hf

[b] Voids only found on sample oxidized at 1,050 °C

iF Oxide-imprinted interfacial areas

+ Standard deviation greater than P_{iF} means only fractions of the interface contained P

– No voids detected in the scratch-induced spallation area

(a) In systems where S segregation took place, the amount at the interface depended on the substrate S content. This can be seen from the NiPtAl coatings on the two AM1 alloys, and also from the high level of S on the PWA1484, whose bulk sulfur content was several times higher than the other superalloys.
(b) Pt in the NiAl coating prevented S segregation, but only when the substrate contained Hf, as in the case of CMSX4; the same was not true with the standard-S AM1, even though the two substrates had the same level of sulfur impurity.
(c) S segregated on the NiAl coating on CMSX4, even though the substrate contained Hf.
(d) Hafnium in PWA1484 did not prevent S segregation.
(e) Yttrium in the NiCoCrAlY coating prevented S segregation, but those interfaces had P.
(f) Enhanced interfacial S segregation took place with excess Cr at the interface; this was observed with the NiPtAl/AM1(s-S) coating after prolonged oxidation to be associated with γ' phases and Cr-rich precipitates.
(g) The amounts of S segregated at interfaces were always significantly lower than those at nearby interfacial void faces, unless there was co-segregation with Cr.

It is unfortunate that the sulfur and other impurity contents in the coatings were never reported and the information was not available. Therefore, when comparing these segregation behaviors, one had no choice but to rely only on the sulfur level in the substrates. This could be a serious problem, even though the above summary shows some interesting relationships between S segregation and the composition of the substrates. Another area of concern, which will not be discussed due to the lack of fundamental knowledge of segregation in multi-component systems, is the fact that several elements, other than sulfur, were enriched at many of these TGO/coating interfaces. These include Cr, Co, Ti, N, sometimes Pt and sometimes perhaps Re as well. How do all these elements affect S segregation or the interface strength is unknown and difficult to address, but are real issues that cannot be ignored in future studies. To date, only Cr and S interactions have been documented [3, 14, 34], an example is also seen in Fig. 11, but whether any other relationships exist between the rest of the segregands with S is not entirely clear.

The results presented in this study, when only the substrate impurity level is being considered, point to different degrees of effectiveness of Pt, Y, and Hf in preventing S segregation, and also some apparent synergisms between Hf and Pt. The type of substrate and its purity level also had a strong effect, as often inferred by cyclic oxidation testing [28, 35, 36]. The fact that the level of S at interfaces was always lower than that on void faces is expected, since the void face is essentially a free surface under the TGO. Segregation to free surfaces are often more favorable than to grain boundaries or to interfaces [37].

Effect of Cr and alloy S content

Before discussing the effects of Pt, Y, and Hf, it is useful to first note the role of Cr. In all of the coatings investigated, Cr was present in the coating and often enriched at the interface. For the NiPtAl boncoats, Cr diffused into the coatings from the substrate starting from the aluminizing process and continued throughout oxidation [25]. Sulfur and Cr are known to co-segregate to surfaces and grain boundaries [38]. Similar co-segregation has been found at Al_2O_3/alloy interfaces for FeCrAl [3, 34], NiCrAl [3] and Cr-containing γ/γ'-NiAl [14]. Part of this apparent co-segregation may be associated with nano-sized Cr

precipitates at the interface, as that seen in Fig. 6 for the NiPtAl bondcoat. However, the depth profile in Fig. 12 and the lack of any observable Cr particles by TEM after this short oxidation time suggests that true segregation due to attractive chemical interaction between Cr and S can also take place. In the simplest term, this amounts to an interaction parameter added to the segregation energy, making segregation more favorable [3]. Since the amount of a segregand at the surface, or interface, is proportional to its concentration in the bulk and to the segregation energy in that $X_{iF} \sim X_{alloy} \exp(-\Delta G/RT)$, any change in the segregation energy, ΔG, can significantly affect the interface concentration, X_{iF}. Likewise, a higher bulk concentration, X_{alloy}, will lead to a higher X_{iF}. This relationship between X_{alloy} and X_{iF} has been demonstrated by the uncoated PWA1484, which had the highest S level compared with other superalloys, and also by the two NiPtAl coatings on the standard versus the low-S AM1 alloys.

Higher interfacial S contents led to much weaker interfaces. This is not only noted by the degree of TGO spallation during cooling, but also demonstrated by the amount of oxide spalled under the scratch motion, as seen in Fig. 17 and Table 3. Porosity at the interface undoubtedly affected adhesion as well. Its effect can be seen by comparing the PWA1484 alloy and the NiPtAl coating on standard-S AM1. Whereas both have similar amounts of interfacial sulfur, the former interface was nearly pore-free, but the latter had a high-pore density, resulting in its much lower strength and extensive spallation during cooling.

Effect of Pt, Hf, and the synergism between them

Comparing NiAl and NiPtAl coatings on the same superalloy, CMSX4, it is clear that Pt prevented S segregation to these TGO/coating interfaces. This result agrees with studies made on model β-NiAl and NiPtAl alloys, where additions of Pt from a few percent to up to 15% eliminated the segregation of S after oxidations at 1,000–1,150 °C from bulk alloys whose S content was about 3 ppm [18]. For the model β-NiAl alloys, the amount of S found at the interface was (2.2 ± 0.5) at.% [6, 18], which is slightly higher but comparable to that found on the NiAl coating. When the NiPtAl coating was deposited on the standard-S AM1 alloy, whose bulk S content was the same as that in CMSX4, Pt no longer prevented S segregation. Only when the AM1 alloy had very low levels of S was the segregation stopped. Results on the standard-S AM1, where high levels of interfacial S were detected along with interfacial Cr enrichment, seem to suggest that the effect of Pt in reducing S segregation is not strong, but can be overwhelmed by the co-segregation of Cr. The same had been observed on a set of γ/γ' Ni-22Al alloys with or without 5% Pt and/or Cr additions [14]. While Pt reduced the degree of interface S segregation, Cr enhanced it even in the presence of Pt.

Why then did Pt in the NiPtAl on CMSX4 prevent S segregation even in the presence of interfacial Cr enrichment? The most obvious difference between CMSX4 and AM1 is the presence of Hf in the former but not in the latter. Perhaps Hf in the alloy diffused into the coating and then exerted an effect. However, from the fact that S was found on the NiAl coating on CMSX4 and on the PWA1484 superalloy, which also contained Hf, it is clear that Hf alone was not sufficient to stop S segregation to these TGO/coating or TGO/alloy interfaces. Yet when Pt was present in the coating and Hf was in the alloy, S segregation was stopped, suggesting that a combination of Pt and Hf were needed on these coatings to eliminate S segregation, unless the S content in the alloy was already reduced to a very low level, like that on the low-S AM1.

Although Hf in these superalloys was not able to prevent interfacial S segregation, its presence in model γ/γ' and β-NiAls has been shown to be effective, not only in stopping S segregation, but also in increasing the interfacial strength [3, 14]. From cyclic oxidation studies, Hf in model NiAl alloys has also been found to be very beneficial in keeping the scale adherent [35, 39], implying that there was no or little S segregation to their interfaces. However, in MCrAl type alloys or commercial superalloys that always contain some Cr, Hf became less effective than Y [40]. If the role of a reactive element, like Hf and Y, is to reduce the sulfur activity in the alloy, thus affect the segregation energy, then it is not surprising that the effectiveness of Hf is less than that of Y, since Y forms a stronger sulfide [41]. Also, different S and Hf activities may exist in different types of alloys. Furthermore, the presence of Cr, due to its co-segregation tendency with S, may also compete with the effect of Hf in reducing S segregation.

The interplay between Pt, Hf, and Cr and the alloy sulfur concentration can be conceptually understood with the simple segregation equation presented before: $X_{iF} \sim X_{alloy} \exp(-\Delta G/RT)$, where ΔG, the segregation energy, is related to the chemical potential of the segregand in the bulk versus that at the interface. A higher X_{alloy} and a greater ΔG would undoubtedly increase X_{iF}. A reduction in the bulk sulfur activity, as associated with the presence of a reactive element, would decrease ΔG and lower X_{iF}. A positive interaction of S with Cr introduces an additional term to ΔG, thus increases X_{iF}. Any changes in the interface energy, as Pt was suggested to do so in NiPtAl [42], would affect the activity of S at the interface, thus affect ΔG and then X_{iF}. The final level of segregation, i.e., X_{iF}, therefore, is a combination of all these factors.

Strengths of the TGO/coating interface were the highest on the NiPtAl/CMSX4, where Hf was present in the superealloy and S was absent at the interface. Studies on

similar types of coating systems have shown that Hf was segregated at the TGO/coating interface [16]. This presence of Hf must have strengthened the interface further, since the NiPtAl/AM1(s-S) sample also had no detectable amounts of S at the interface, but its interfacial strength was noticeably lower (Fig. 17). The ability of a reactive element to strengthen the interface beyond its role of eliminating S segregation has been suggested before [12, 13], and was recently demonstrated by first principles calculations for the case of Hf in γ-NiAl [7].

Effect of Y and the segregation of P

Yttrium in the NiCoCrAlY coating prevented sulfur segregation to the oxide/coating interface, even though the coating contained Cr and the substrate PWA1484 had a high level of sulfur that segregated readily at the TGO/PWA1484 interface. The ability of Y in preventing interfacial sulfur segregation have been demonstrated in FeCrAlY alloys [43, 44] and recently in a β-Ni40Al5-Cr0.03Y alloy (P. Y. Hou et al., Unpublished results). However, small amounts of sulfur still segregated to void faces on the NiCoCrAlY coating, and on the β-NiAlCrY alloy (P. Y. Hou et al., Unpublished results), with an average level of 1.5 at.%. These results indicate that Y in MCrAlY is sufficient in eliminating S segregation to oxide/alloy interfaces, but not to free surfaces. On the latter, Y only reduced the amount segregated, similar to prior results obtained from in-situ AES studies on MCrAlY alloy surfaces [11, 12, 45]. Many cyclic oxidation studies on superalloys and coatings also showed beneficial effects of Y in improving TGO adhesion [32, 36], suggesting that Y was successful in stopping interfacial S segregation.

The surprise found on the NiCoCrAlY coating studied here was the presence of P at all the interfacial areas examined. Although the coating surface was not polished, it was thoroughly cleaned prior to oxidation. Therefore, the detected P should not have been a surface contaminant. Furthermore, the same cleaning procedure was used on the unpolished NiAl and NiPtAl coatings on CMSX4, but no P was detected there. Small amounts of P on some interfacial areas were occasionally found on the low-sulfur regions on the NiPtAl/AM1(s-S) coating and on the PWA1484 alloy, indicating that P was also a segregand on alloys that were less clean. However, the P level on those interfaces that contained S was always very low and its appearance sporadic. It is therefore possible that while P has a tendency to segregate to the interface, it competes with S such that S segregation dominates. This is a reasonable assertion, since the segregation enthalpy of P, to surfaces and grain boundaries in α-Fe, is about half that of S [46, 47], indicating a weaker segregation tendency. When the coating contains a strong sulfide former like Y, the bulk S activity becomes so reduced that S no longer segregates; then P segregation becomes prevalent. Phosphorus is known to segregate readily to surfaces and grain boundaries and causes grain-boundary embrittlement [48, 49]. There have been no reports indicating the effectiveness of Y in reducing P segregation, but Ti [50] and La [51] are known to reduce the grain-boundary segregation of P in Fe-based alloys. Compare with S, the same amount of P at the interface was less detrimental to the interfacial strength, as seen in Fig. 17. It is not known if P segregated during cooling. Most interfacial S was probably present at the oxidation temperature, since a prior study showed that its level did not change with cooling rates [34]. The same is not yet known for P, but whenever P segregated, since the interfacial strength was tested at room temperature and coated components are often cooled to such low temperatures, its presence at the interface and its detrimental effect on strength are still alarming.

Conclusions

The segregation behavior of sulfur and other elements at TGO/coating interfaces have not been extensively studied. Available results from NiAl, NiPtAl and NiCoCrAlY bondcoats on CMSX4, AM1, or PWA1484 superalloys were presented. It was found that the degree of interfacial sulfur segregation (i) depended on the substrate S content, (ii) increased with co-segregation of Cr at or near the interface, (iii) was significantly lower than that at nearby interfacial void faces unless there was Cr co-segregation, and (iv) dropped to non-detectable levels when Pt was present in the coating along with Hf in the superalloy. Pt alone in the coating without the presence of any reactive element in the substrate was not able to prevent S segregation; neither was Hf alone in the alloy effective without the presence of any Pt. The necessary combination of Pt and Hf in these coatings and alloys is believed to be associated with the presence of Cr, which increases the S segregation tendency. Yttrium was effective in eliminating interfacial S segregation even in the presence of Cr, but did not totally stop the S from segregating to interfacial void faces. Phosphorus was detected everywhere on the TGO/NiCoCrAlY interface. Other than S, P, and Cr, most interfaces were also enriched with Ti, N, and Co, and in one case probably Re as well. Pt in β-NiPtAl seemed to segregate at the interface only when there was no Al enrichment.

Sulfur at the TGO/coating interface greatly reduced its strength. For the same amount, P was less detrimental than S. The presence of Hf in the substrate further strengthened an interface where S was not detected, indicating beneficial effect of Hf on oxide adhesion beyond that of preventing interfacial S segregation.

Acknowledgements The author is grateful for the following people and company for providing samples: Snecma (Safran group) for the NiPtAl on AM1 through Dr. Regine Molins, Mr. Kenneth S. Murphy at Howmet Castings for the NiPtAl on CMSX4 through Dr. Vladimir Tolpygo and Mr. M. Maloney and Mr. D. Litton of Pratt and Whitney for the NiCoCrAlY on PWA1484 through Prof. Kevin Hemker. The permissions from Dr. Regine Molins of Ecole des Mines de Paris and Dr. Vladimir Tolpygo of Honeywell Aerospace to use some of their results from our prior collaborations are greatly appreciated. The Auger studies were performed at the Molecular Foundry, Lawrence Berkeley National Laboratory. Financial supports for the Molecular Foundry and for parts of this work are provided by the Office of Science, Office of Basic Energy Sciences, of the U.S. Department of Energy under Contract No. DE-AC02-05CH11231. This work is also supported in part by AFOSR under the MEANS-2 Program (Grant No. FA9550-05-1-0173).

References

1. Gell M, Vaidyanathan K, Barber B, Cheng J, Jordon E (1999) Metall Mater Trans A 30A:427. doi:10.1007/s11661-999-0332-1
2. Meier SM, Nissley DM, Sheffler KD, Cruse TA (1992) J Eng Gas Turb Power 114:258. doi:10.1115/1.2906581
3. Hou PY (2008) Ann Rev Mater Res 38:275
4. Kiely J, Yeh T, Bonnell DA (1997) Surf Sci 393:L126. doi:10.1016/S0039-6028(97)00786-3
5. Zhang W, Smith JR, Wang XG, Evans AG (2003) Phys Rev B 67:245414. doi:10.1103/PhysRevB.67.245414
6. Hou PY, Priimak K (2005) Oxid Met 63:113. doi:10.1007/s11085-005-1954-3
7. Smith JR, Jiang Y, Evans AG (2007) Int J Mater Res 12:1214
8. Hayashi S, Wang W, Sordelet DJ, Gleeson B (2005) Metall Mater Trans A 36:1769. doi:10.1007/s11661-005-0041-3
9. Whittle DP, Stringer J (1980) Philos Trans R Soc Lond A 295:309. doi:10.1098/rsta.1980.0124
10. Pint BA (2001) In: Tortorelli P, Wright IG, Hou PY (eds) Proceedings of the John Stringer symposium on high temperature corrosion, ASM International, OH, p 52
11. Funkenbusch W, Smeggil JG, Bornstein NS (1985) Metall Trans 16A:1164
12. Smialek JL, Browning R (1985) In: Munir ZA, Cubicciott D (eds) Proceedings of the Symposium in High Temperature Materials Chemistry III, vol 82-2. The Electrochemical Society, PA, p 258
13. Hou PY (1999) Oxid Met 52:337. doi:10.1023/A:1018899729758
14. Hou PY, Isumi T, Gleeson B (2008) Oxid Met (in press)
15. Felten EJ (1976) Oxid Met 10:23. doi:10.1007/BF00611696
16. Haynes JA, Pint BA, More KL, Zhang Y, Wright IG (2002) Oxid Met 58:513. doi:10.1023/A:1020525123056
17. Cadoret Y, Bacos M-P, Josso P, Maurice V, Marcus P, Zanna S (2004) Mater Sci Forum 461–464:274
18. Hou PY, McCarty KF (2006) Scr Metab 54:937. doi:10.1016/j.scriptamat.2005.10.065
19. Warnes BM, Punola DC (1997) Surf Coat Technol 94–95:1. doi:10.1016/S0257-8972(97)00467-2
20. Hou PY, Tolpygo VK (2007) Surf Coat Technol 202:623. doi:10.1016/j.surfcoat.2007.06.013
21. Meier SM, Nissley DM, Sheffler KD (1991) Report vol 189111, National Aeronautics and Space Administration, Cleveland, OH
22. Hou PY (1998) In: Hou PY, McNallan MJ, Oltra R, Opila EJ, Shores DA (eds) High temperature corrosion and materials chemistry, The Electrochemical Society, Pennington, p 198
23. Molins R, Hou PY (2006) Surf Coat Technol 201:3841. doi:10.1016/j.surfcoat.2006.07.251
24. Davis LE, MacDonald NC, Palmbery PW, Riach GE, Weber RE (1976) Handbook of auger electron spectroscopy, 2nd edn. Physical Electronics Division, Perkin-Elmer Corporation, Minnesota
25. Molins R, Guerre C, Remy L (2003) Rev Metallurgie 100:507
26. Molins R, Rouzou I, Hou PY (2006) Oxid Met 65:263. doi:10.1007/s11085-006-9019-9
27. Chieux M, Molins R, Remy L, Duhamel C, Sennour M, Cadoret Y (2008) Proceedings of the 7th International Symposium on High Temperature Corrosion and Protection of Materials. Les Embiez, France
28. Molins R, Rouzou I, Remy L, Le Biavant-Guerrier K, Jomard F (2005) Mater High Temp 22:359. doi:10.3184/096034005782744083
29. Mendis BG, Tryon B, Pollock TM, Hemker KJ (2006) Surf Coat Technol 201:3918. doi:10.1016/j.surfcoat.2006.07.249
30. Hindam H, Whittle DP (1982) J Electrochem Soc 129:1147. doi:10.1149/1.2124044
31. Whittle DP, Schaffer S, Boone DH (1981) Thin Solid Films 84:73. doi:10.1016/0040-6090(81)90011-0
32. Toscano J, Vaen R, Gil A, Subanovic M, Naumenko D, Singheiser L et al (2006) Surf Coat Technol 201:3906. doi:10.1016/j.surfcoat.2006.07.247
33. Hemker KJ, Mendis BG, Livi KJT (2006) Scr Mater 55:589. doi:10.1016/j.scriptamat.2006.06.017
34. Hou PY (2000) Mater Corros 51:329. doi:10.1002/(SICI)1521-4176(200005)51:5<329::AID-MACO329>3.0.CO;2-K
35. Pint BA, Wright IG, Lee WY, Zhang Y, Prüßner K, Alexander KB (1998) Mater Sci Eng A 245:201
36. Haynes JA, Pint BA, Zhang Y, Wright IG (2007) Surf Coat Technol 202:730. doi:10.1016/j.surfcoat.2007.06.039
37. Johnson WC, Blakely JM (eds) (1997) Interfacial Segregation. ASM, Materials Park
38. Uebing C (1996) Prog Surf Sci 53:297. doi:10.1016/S0079-6816(96)00027-5
39. Lzumi T, Gleeson B (2006) Mater Sci Forum 522–523:221
40. Sarioglu C, Stiger MJ, Blachere JR, Janakiraman R, Schumann E, Ashary A et al (2000) Mater Corros 51:358. doi:10.1002/(SICI)1521-4176(200005)51:5<358::AID-MACO358>3.0.CO;2-C
41. Sigler DR (1989) Oxid Met 32:337. doi:10.1007/BF00665442
42. Gauffier A, Saiz E, Tomsia AP, Hou PY (2007) J Mater Sci 42:9524. doi:10.1007/s10853-007-2093-9
43. Tolpygo VK, Viefhaus H (1999) Oxid Met 52:1. doi:10.1023/A:1018818906559
44. Mennicke C, Schumann E, Al-Badairy H, Tatlock GJ, Goebel M, Borchardt G et al (1998) Phys Status Solidi A 167:419. doi:10.1002/(SICI)1521-396X(199806)167:2<419::AID-PSSA419>3.0.CO;2-E
45. Briant CL, Luthra KL (1988) Metall Trans 19A:2099
46. Grabke HJ (1986) Steel Res 57:178
47. Bradley JR, Aaronson HI, Russell KC, Johnson WC (1977) Metall Trans A 8A:1955
48. LejEek P, Krajnikov AV, Ivashchenko YN, Militzer M, Adamek J (1993) Surf Sci 280:325. doi:10.1016/0039-6028(93)90685-D
49. Nikolaeva AV, Nikolaev YA, Kevorkyan YR (2001) At Energy 91:2325
50. Viefhaus H, Richarz B (1995) Mater Corros 46:306. doi:10.1002/maco.19950460506
51. Hong SH, Kang SJ, Yoon DN, Baek WH (1991) Metall Trans A 22A:2969. doi:10.1007/BF02650256